Digest Journal of Nanomaterials and Biostructures Vol. 10, No. 1, January - March 2015, p. 265 - 275

STRUCTURAL, ELECTRICAL AND DIELECTRIC BEHAVIOR OF $Ni_xCo_{1-x}Nd_yFe_{2-y}O_4$ NANO-FERRITES SYNTHESIZED BY SOL-GEL METHOD

M. T. FARID[a*], I. AHMAD[a], S. AMAN[a], M. KANWAL[a], G. MURTAZA[a], I. ALI[a], I. AHMAD[b], M. ISHFAQ[a]
[a]*Department of Physics, Bahauddin Zakariya, University Multan, 60800. Pakistan*
[b]*Institute of Chemical Sciences, Bahauddin Zakariya, University Multan, 60800, Pakistan*

The influence of neodymium (Nd) contents on the structural, electrical and dielectric properties of Nickel cobalt ferrites was studied in the ferrite series $Ni_xCO_{1-x}Nd_yFe_{2-y}O_4$ (x= 0.00, 0.20, 0.40, 0.60, 0.80, 1.0 and y = 0.00, 0.02, 0.04, 0.06, 0.08, 0.1). This series was prepared by sol-gel method. XRD analysis reveals single phase samples up to y=0.04. At y ≥ 0.06, a secondary phase of iron neodymium oxide ($NdFeO_3$) appears along with the spinel phase. The incorporation of Nd^{3+} for Fe^{3+} ions results in a slight increase of lattice constant due to larger ionic radius of the substituted ions. It was inferred that the substitution of neodymium limits the grain growth. The DC electrical resistivity and activation energy are higher for the substituted samples. The dielectric constant, dielectric loss (tan δ) and AC-conductivity decreased on account of doping. The decrease in dielectric constant is imputed to the reduction in the internal viscosity of the doped samples. The dielectric data are explained on the basis of space charge polarization. Ferrites have high dielectric constant and low tan δ, they may be attractive for application in switching and memory storage devices.

(Received February 6, 2015; Accepted March 20, 2015)

Keywords: Solgel method, Nd, Cubic spinel Ferrites, dc resistivity, Dielectric properties

1. Introduction

In recent years many studies have been focused on the synthesis of nanometal oxides because of their unusual optical, electrical and magnetic properties than that of their bulk counterpart [1]. Spinel ferrites, MFe2O4 (M=Mn, Co, Zn, Mg, etc.), are a family of oxide materials with great technological importance and can be used in the fabrication of magnetic, high frequency transformers, antennae and various microwave and radar devices [2]. The ferrites behave as inhomogeneous dielectric materials in which individual high-conducting grains are separated by either air gaps or low-conducting layers. Due to high resistivity, low eddy current losses and convincingly low costs coupled with their potential microwave applications such as circulators, isolators and phase shifters, lithium ferrites have fascinated considerable interest for many researchers [3]. Cobalt ferrite has a partially inverse spinel structure in which both sites, i.e. tetrahedral (A) and octahedral (B) sites, contain a fraction of Co^{2+} and Fe^{3+} cations; however it is generally accepted that a large fraction of Co^{2+} ions are on the B-site and the remaining are on the A-site, which depends on the production methods as well as on the heat treatment procedure [4–6]. Rare earth ions have unpaired 4f electrons. The fourth shell ions are shielded by the ions in the fifth shell and are hardly affected by the potential field of the surrounding ions [7]. By introducing rare earth ions into the system, the Nd^{3+}–Fe^{3+} interactions appear (3d–4f coupling) which affect the electrical and magnetic properties of the spinel ferrites. Substitution of rare earth ions into the

* Corresponding author: tahir95263@yahoo.com

spinel structure lead to structural distortion which modify the electrical transport properties. Studies concerning the effects of substitution of Tb, Dy, Yb, Er, Gd, Sm, Ce, Y, Eu, La, Th, etc., in various spinel ferrites have been carried out by several researchers [8–10]. Incorporation of various substitutions and different molar ratios in Ni–Co ferrite was studied [11, 12]. Substitution of rare earth ion into the spinel structure shows structural distortion [13–15] inducing strain in the sample with significant change in the electrical and magnetic properties. The structural, dielectric and transport properties of rare earth doped Ni ferrite were reported by Dwevedi et al. [16].

The purpose of the investigation is to study the effect of Neodymium ions substitution for nickel cobalt ions on structural, electrical and dielectric properties of $Ni_xCO_{1-x}Nd_yFe_{2-y}O_4$ ferrites to make these ferrites suitable for switching and memory storage devices applications.

2. Materials and methods

$Ni_xCO_{1-x}Nd_yFe_{2-y}O_4$ (x= 0.00, 0.20, 0.40, 0.60, 0.80, 1.0 and y = 0.00, 0.02, 0.04, 0.06, 0.08, 0.1) nano ferrites were synthesized by sol–gel auto-combustion technique. Analytical grade Co $(NO_3)_2$, Ni $(NO3)_2$, Fe_3Cl_2 and Nd_2O_3 (99.99% pure) were dissolved initially in 100 ml de-ionized water in a Pyrex beaker. To obtain homogenous and transparent solution, citric acid was used as a chelating agent. Dissolved solution was mixed homogeneously by placing it on magnetic stirrer at the temperature of 80 ^oC . pH value was maintained at 7–8 by adding ammonia solution continuously followed by stirring for 6–7 hours. The solution transformed into viscous gel first and then a self combustion phenomenon occurred at temperature 370 ^oC. Dry gel converted into fluffy powder called ‘‘precursor powder’’ after its complete burning. The powder, after complete grinding, was then pre-sintered at 700 ^oC in a furnace for 5 hours, followed by furnace cooling. These sintered powders were then pressed into pellets under the load of (~30 KN) by using Paul–Otto Weber Hydraulic Press. The pellets were formed using (3–5 wt %) polyvinyl alcohol as a binder. The binder was evaporated at 250 ^oC for 1 hour and finally samples were sintered again at 950 ^oC for 7 hours.

The structural characterization of all the samples was carried out by the X-ray diffraction. XRD data were taken at room temperature using CuK_α (λ = 1.5406A°) radiation. dc electrical resistivity for all these samples was measured by two-probe method. The electrical resistivity was measured with sample pellet of 2.0 mm thickness and 13mm diameter. For dielectric measurements silver paint was applied on both sides of the pellets and air dried to have good ohmic contact. The dielectric measurements were made using a precision LCR meter (Wayne Kerr LCR 4275) at room temperature in the frequency range 1 MHz to 3 GHz.Using LCR meter the dielectric parameters such as Capacitance of the pellet, tan δ (loss tangent) and Capacitance of air with the same thickness as the pellet were measured. The real part of dielectric constant (ε') was determined from the following formula.

$$\varepsilon' = \frac{C_p}{C_{Air}} \tag{1}$$

Where ε'= Real part of dielectric constant
C_p = Capacitance of the Pellet in Faraday
C_{Air} = Capacitance of Air in Faraday

The imaginary part of the dielectric constant (ε'') or dielectric loss was measured by using the following relation.

$$\varepsilon'' = \varepsilon' \tan\delta \tag{2}$$

ε'= Real part of dielectric constant
tan δ = loss tangent

3. Results and Discussion

3.1 X-ray studies

X-ray diffraction patterns of $Ni_xCO_{1-x}Nd_yFe_{2-y}O_4$ (x= 0.00, 0.20, 0.40, 0.60, 0.80, 1.0 and y = 0.00, 0.02, 0.04, 0.06, 0.08, 0.1) ferrite system are shown in Fig. 1.

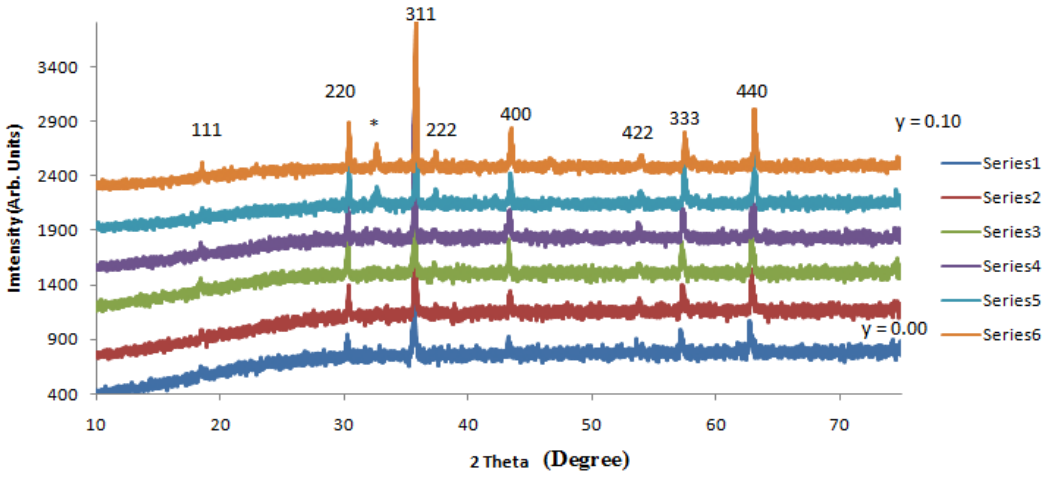

Fig. 1. X-Ray Diffraction patterns of $Ni_xCO_{1-x}Nd_yFe_{2-y}O_4$ ferrites

All the samples show good crystallization, with well-defined diffraction peaks. Table 1 shows the composition of the phases precipitated and the lattice constants of the $Ni_xCO_{1-x}Nd_yFe_{2-y}O_4$ ferrites. For y =0.04, the samples have the monophase cubic spinel structure while for y ≥0.06, the samples are biphasic. The presence of the strong diffraction peaks corresponding to the planes (111), (220), (311), (222), (400), (422), (511/333), (440) indicates the presence of cubic spinel phase. Miller indices (h k l) and inter-planer spacing (d) for $Ni_xCO_{1-x}Nd_yFe_{2-y}O_4$ ferrites system are listed in Table 1.

Table 1. Phases, lattice constant, X-ray density and grain size of $NixCO1_{-x}Nd_yFe_{2-y}O_4$ (x= 0.00, 0.20, 0.40, 0.60, 0.80, 1.0 and y = 0.00, 0.02, 0.04, 0.06, 0.08, 0.1) ferrite.

Composition	**Secondary Phase**	**Lattice Parameter a(°A)**	**X-ray density (g/cm^3)**	**Grain Size (nm)**
$COFeO_4$	-----	8.363	5.376	8.48
$Ni_{0.20}CO_{0.80}Nd_{0.02}Fe_{0.98}O_4$	-----	8.368	5.423	7.36
$Ni_{0.40}CO_{0.60}Nd_{0.04}Fe_{0.96}O_4$	-----	8.371	5.457	6.80
$Ni_{0.60}CO_{0.40}Nd_{0.06}Fe_{0.94}O_4$	$NdFeO_3$	8.375	5.489	5.30
$Ni_{0.80}CO_{0.20}Nd_{0.08}Fe_{0.92}O_4$	$NdFeO_3$	8.38	5.524	3.86
$NiNd_{0.10}Fe_{0.90}O_4$	$NdFeO_3$	8.384	5.571	3.03

A peak corresponding to 2□=33.1° (indicated by * in Fig. 1) is attributed to secondary phase at the grain boundaries and appears for y ≥0.06 and magnitude of intensity increases with the increase of Neodymium concentration. This peak is identified as $FeNdO_3$ (iron neodymium oxide) matched with ICDD PDF # 39-1489. The secondary phase on the grain boundaries appears due to high reactivity of Fe^{3+} ions with Nd^{3+} ions [17]. The lattice constant (a) increases slightly for all the compositions is shown in fig. 2.

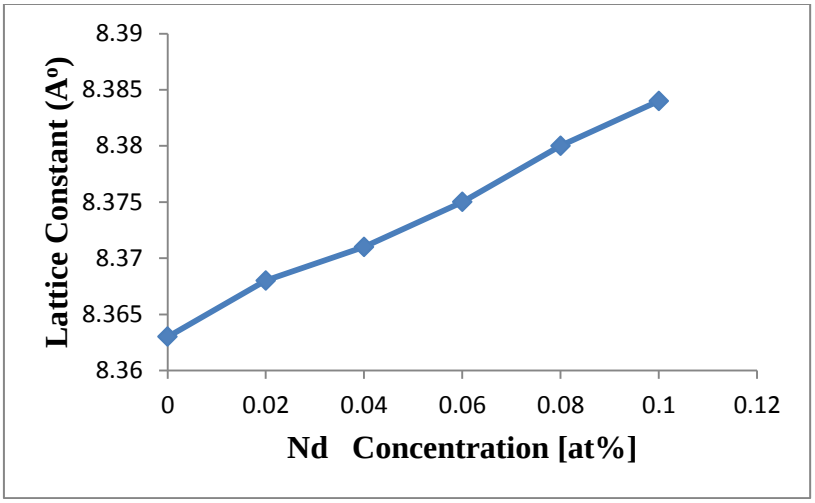

Fig. 2. Lattice Constant 'a' as a function of Nd Concentration x at.%

The variation can be explained on the basis of ionic radii of the substituted ions. The replacement of the smaller Fe^{3+} ions (0.64 °A) with larger Nd^{3+}ions (0.983 °A) causes dilation of the host spinel lattice which results in the increase of lattice constant. This observation is consistent with the results reported by various authors where it has been reported that the substitution of rare earth ions increases the lattice constant [18, 19]. The lattice parameter for biphasic samples still increases with Neodymium contents which enables us to conclude that the spinel lattice is not compressed by the secondary phase. Thus, there is no solubility limit for Neodymium ions (rare-earth transition metal) inthese ferrite in the given range ($y \geq 0.12$). Such observation in the lattice constant in rare-earth substituted ferrites has been reported by Hemeda et al. [20] in case of $NiGd_xFe_{2-x}O_4$. The measured particle size of all the samples by Scherrer's formula [21] is given in Table 1.

$$D = \frac{0.9\lambda}{\beta \cos\theta} \tag{3}$$

Where β is the full width half maximum (rad), λ the wavelength of the X-ray, θ the angle between the incident and diffracted beams (degree) and *D* the particle size of the sample (nm). This confirms that the citric acid is more effective burning agent for producing fine ferrite powder with sol–gel auto combustion method. Homogeneity of the chemical composition of the ferrite particles was acquired by thermal decomposition of nitrates.
The x-ray density of the samples is calculated by relation,

$$\rho_x = \frac{8M}{Na^3} \tag{4}$$

Where M is the molecular weight of the sample, N the Avogadro's number and a^3 the volume of the cubic unit cell.

3.2. Electrical properties

Room temperature dc resistivity measured by two probe method as a function of Nd-concentration are reported in Fig. 3 which clearly demonstrating the increasing trend of resistivity with increase in Nd concentration.

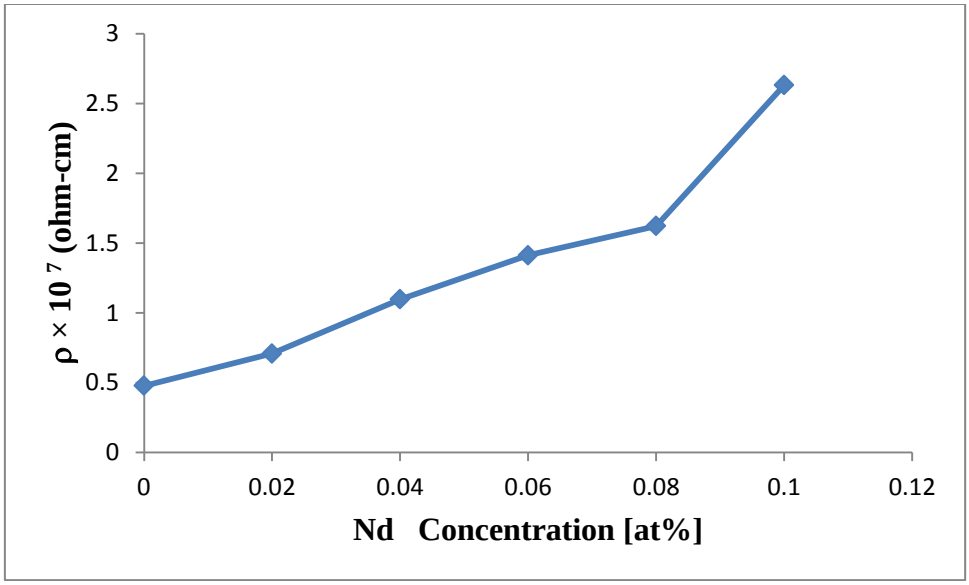

Fig. 3. The log of room temperature dc resistivity as a function of Nd-Concentration x at.%

In $Ni_xCO_{1-x}Nd_yFe_{2-y}O_4$ (x= 0.00, 0.20, 0.40, 0.60, 0.80, 1.0 , y = 0.00, 0.02, 0.04, 0.06, 0.08, 0.1) alloys, the concentration of Fe^{3+} ions on Octahedral sites gradually decreases with increasing x while the substituted Nd^{3+} partially occupies the corresponding empty location. As the Nd^{3+} ions has large ionic radius which may be one of the causes to decrease the hopping rate of electron as it enhances the separation between Fe^{2+} and Fe^{3+} ions and consequently, enhances the dc resistivity and activation energy. These results are consistent with the results reported by various authors [24, 25]. Similar results with Dy doping in Ni-Co ferrites has been reported by [26]. The temperature dependent dc resistivity measured using two probe method in the temperature range 303 -573 K for $Ni_xCO_{1-x}Nd_yFe_{2-y}O_4$ (x= 0.00, 0.20, 0.40, 0.60, 0.80, 1.0 , y = 0.00, 0.02, 0.04, 0.06, 0.08, 0.1), as a function of temperature are given in Fig. 4 .

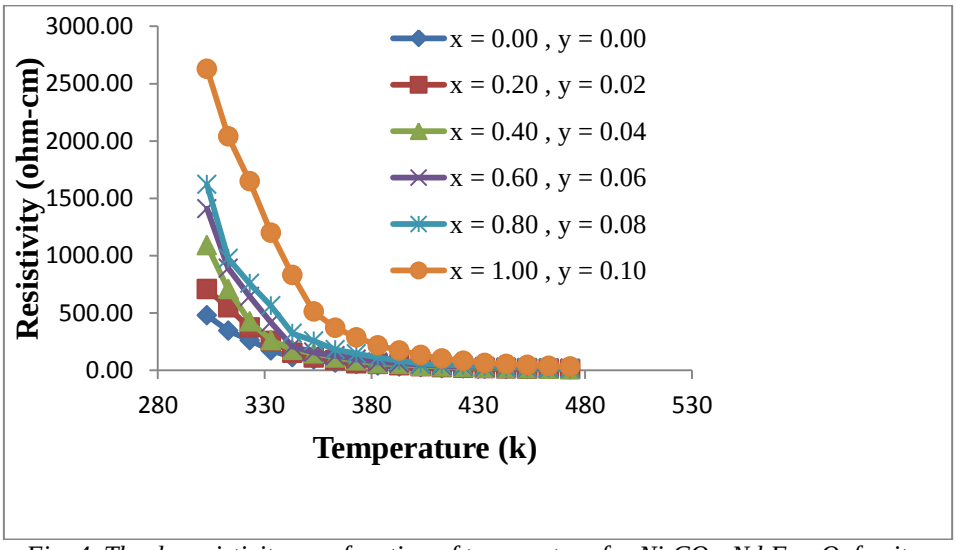

Fig. 4. The dc resistivity as a function of temperature for $Ni_xCO_{1-x}Nd_yFe_{2-y}O_4$ ferrites

These graphs show that the increase in temperature leads to decrease in resistivity which is the normal behavior of semiconducting materials and it obeys the well known Arrhenius relation [27]. The higher values of temperature for the samples help the trapped charges to be librated and participate in the conduction process which results decrease in resistivity. According to the

conduction mechanism in ferrites, the decrease in resistivity could also be related to the increase in the drift mobility of the thermally activated electrons [28, 29].
Drift mobility (μ_d) is calculated from electrical resistivity data using the following relation [30–32]:

$$\mu_d = \frac{1}{ne\rho} \tag{5}$$

Where e is the charge of electron, ρ is electrical resistivity and n is the concentration of charge carriers and can be calculated using following equation:

$$n = \frac{N_A C_{Fe} \rho_b}{M} \tag{6}$$

Where N_A is the Avogadro's number, C_{Fe} the number of iron atoms in the chemical formula of the samples, ρ_b the bulk density and M is the molar mass of the samples. Fig. 5 shows the variation of drift mobility with temperature.

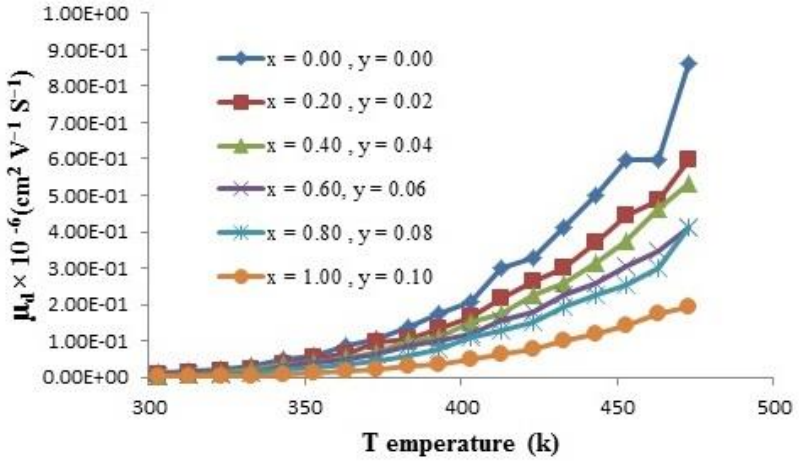

Fig. 5. Drift mobility as a function of temperature for $Ni_xCO_{1-x}Nd_yFe_{2-y}O_4$ ferrites

It is observed that the drift mobility increases with the increase in temperature. This is due to the fact that the charge carriers start hopping from one site to another as the temperature increases.

3.3. Dielectric properties

3.3.1. Compositional effect on electrical permittivity

The variation of dielectric constant and complex dielectric constant determined vs frequency for $Ni_xCO_{1-x}Nd_yFe_{2-y}O_4$ (x= 0.00, 0.20, 0.40, 0.60, 0.80, 1.0 and y = 0.00, 0.02, 0.04, 0.06, 0.08, 0.1) ferrites at room temperature are shown in Figs. 6 and 7 respectively.

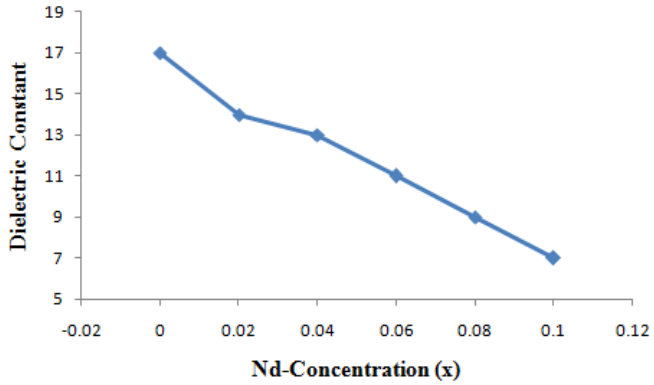

Fig. 6. Dielectric constant vs Nd-concentration (x) for $Ni_xCO_{1-x}Nd_yFe_{2-y}O_4$ ferrites

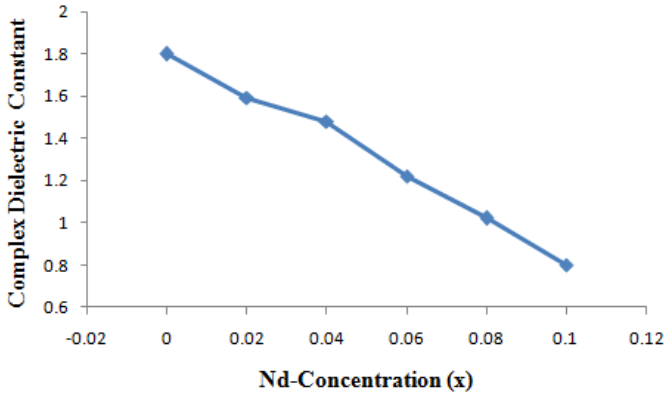

Fig. 7. Complex Dielectric constant vs Nd-concentration (x) for $Ni_xCO_{1-x}Nd_yFe_{2-y}O_4$ ferrites

It can be seen from the figures 6 and 7 that both ε' and ε'' decrease with the increase of Neodymium concentration. It was observed that the electronic exchange between Fe^{2+} and Fe^{3+} results in local displacements, determining the polarization of charges in these ferrites. Thus, it is the number of ferrous ions on octahedral sites that play a dominant role in the process of conduction and dielectric polarization. Due to larger ionic radius, Nd^{3+} ions occupy octahedral sites [33]. The concentration of Fe^{3+} ions at B-sites decreases gradually with increasing concentration of Neodymium up to y = 0.02. At y> 0.02, the reduction in the values of dielectric constant and complex dielectric constant with increasing concentration of Neodymium is due to depicting concentration of iron ions at B-sites which play a dominant role in dielectric polarization due to the presence of second phase. The electron transfer between Fe^{2+} and Fe^{3+} ions will be hindered i.e. the polarization decreases. Consequently, both dielectric (ε') and complex dielectric constant (ε'') decrease with Neodymium contents[34].

3.3.2. Effect of frequency on dielectric and complex dielectric constant

At room temperature, the real and imaginary part of dielectric constant (ε' and ε'') of $Ni_xCO_{1-x}Nd_yFe_{2-y}O_4$(x= 0.00, 0.20, 0.40, 0.60, 0.80, 1.0, y = 0.00, 0.02, 0.04, 0.06, 0.08, 0.1) as a function of frequency in the range of 1 MHz to 3GHz were studied and results had been plotted in figures 8 and 9.

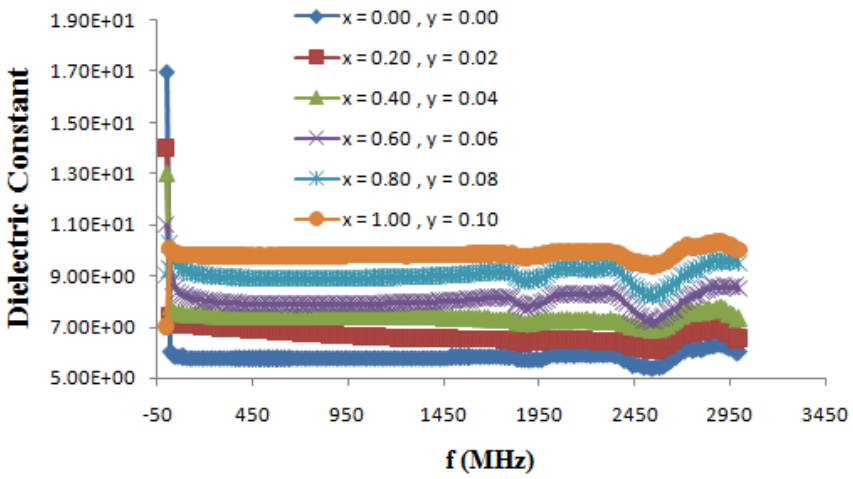

Fig. 8. Dielectric constant vs frequency (MHz) for $Ni_xCO_{1-x}Nd_yFe_{2-y}O_4$ ferrites

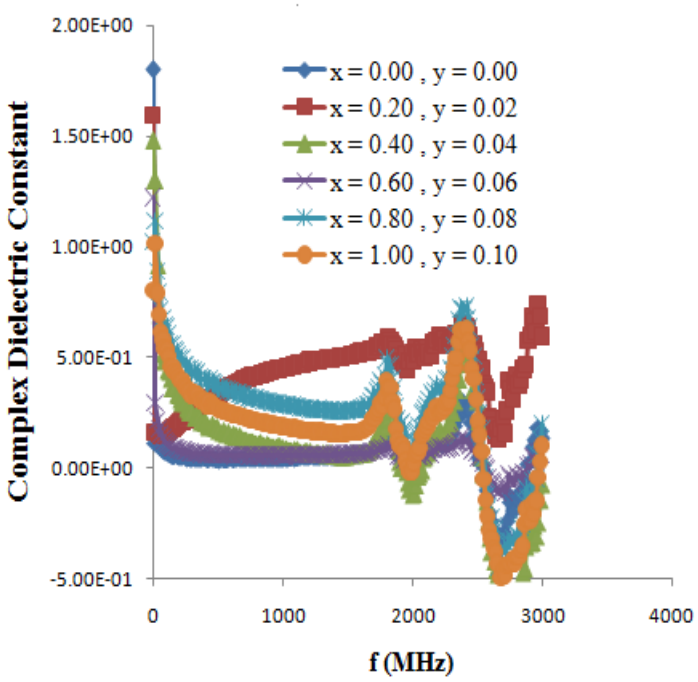

Fig. 9. Complex Dielectric constant vs frequency (MHz) for $Ni_xCO_{1-x}Nd_yFe_{2-y}O_4$ ferrites

At high frequency, the values of ε' and ε'' are almost constant. Similar results were observed by [35]. From graphs, it is clear that all the samples have higher dielectric constant at lower frequency. The decrease in ε' is sharp initially at lower frequency and then ε' value decreases slowly with the increase in frequency and showed almost frequency independent behavior at high frequency regions, similar behavior was observed by [36]. The variation of dielectric constant with frequency may be explained on the basis of space-charge polarization phenomenon[37]. According to space-charge polarization phenomenon, dielectric material has well conducting grains, which are separated with highly resistive grain boundaries. When electric field is applied, space charge accumulates at the grain boundaries and voltage drops mainly at grain boundaries. Koops proposed that grain boundary affect is more at low frequencies [38]. When the frequency given to dielectric material is increased beyond a specific limit the electron exchange between Fe^{2+} and Fe^{3+} ions does not follow the variations of applied field, and the value of dielectric constant almost becomes constant. According to Maxwell and Wagner [39] two layer model, the dielectric structure of ferrite material is assumed to be made of two layers. First layer is a conducting layer,

which consist of large conducting ferrite grains separated by other thin weakly conducting intermediate grain boundaries. [40] pointed out that polarization in ferrites is through a mechanism, which is similar to the conduction process. The exchange of electron between ferrous and ferric ions, results in local displacement of electrons in the direction of field that is applied to the dielectric material determines polarization. As the frequency increases, the Polarization decreases and then approaches a constant value. The fact behind that behavior is that, when applied field increases a specific frequency of external field, the electron exchange $Fe^{2+} \leftrightarrow Fe^{3+}$ cannot follow the alternating field. The high value of dielectric constant at lower frequency is due to the predominance of the species like Fe^{2+} ions, oxygen vacancies, grain boundary defects, etc while the decrease in dielectric constant with frequency is natural that is any species contributing to the polarizability is found to show the applied field lagging behind at higher frequencies[41].

3.3.3. Loss Tangent (tan δ)

The loss tangent is a parameter of a dielectric material that quantifies its inherent dissipation of electromagnetic energy at different frequencies. It measures the loss of electrical energy from the applied electric field into the samples at different frequencies.

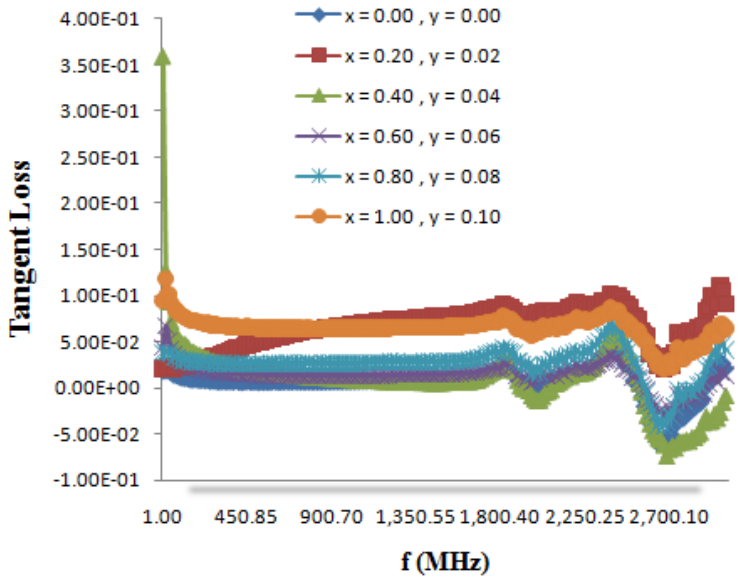

Fig.10. Tangent loss vs frequency (MHz) for $Ni_xCO_{1-x}Nd_yFe_{2-y}O_4$ ferrites

Fig. 10 shows that the loss decreases rapidly in the low frequency region while the rate of decrease is slow in high-frequency region and it shows an almost frequency independent behavior in high frequency region. The behavior can be explained on the basis that in the low frequency region, which corresponds to a high resistivity (due to the grain boundary), more energy is required for electron exchange between Fe^{2+} and Fe^{3+} ions, as a result the loss is high. In the high frequency region, which corresponds to a low resistivity (due to the grains), small energy is required for electron transfer between the two Fe ions at the octahedral site. Moreover, the dielectric loss factor also depends on a number of factors such as stoichiometry, Fe^{2+} content, and structural homogeneity which in turn depend upon the composition and sintering temperature of the samples [42]. Also it is known that there is strong correlation, between the conduction mechanism and the dielectric constant behavior (Polarization mechanism) in ferrites. At high frequencies the peaking behavior is observe. This type of peaking behavior (Debye-type relaxation) is observed when the jumping frequency of the Fe^{+2} and Fe^{+3} ions is exactly equal to the frequency of the applied field [37] i.e.

$$\omega\tau = 1 \qquad (7)$$

Where τ is the relaxation time of hopping process and ω is the angular frequency of the field. This shows that with increase in Nd concentration the energy losses decrease at high frequencies. The low loss values at higher frequencies show the potential applications of these materials in high frequency micro wave devices.

4. Conclusions

We have successfully synthesized single phase $Ni_xCo_{1-x}Nd_yFe_{2-y}O_4$ nano ferrites with cubic spinel structure through sol-gel method with very fine crystallite size in first three samples, while secondary phase is observed when $y \geq 0.06$.

dc resistivity increases with the increase in neodymium concentration, and with the increase in temperature, dc resistivity decreases which proves the semiconducting materials.

A normal dispersion in dielectric parameters (ε', ε", tan δ) with frequency was observed for all samples and this has been explained on the basis of space charge polarization mechanism as discussed in Maxwell-Wagner model.

Low values of conductivity around room temperature indicate that the studied compositions may be good candidates for the microwave applications that require negligible eddy currents.

All the samples showed a decreasing trend in tan δ with increase in frequency which is normal behavior of any ferrite materials. At high frequency, the peaking behavior is observed. This type of peaking behavior (Debye-type relaxation) is observed when the jumping frequency of the Fe^{+2} and Fe^{+3} ions is exactly equal to the frequency of the applied field.

The values of dielectric loss tangent decreases, this shows that with increase in Nd concentration in Ni-Co nano ferrites the energy losses decrease at high frequencies. The low loss values at higher frequencies show the potential applications of these materials in high frequency micro wave devices.

References

[1] D.H. Chen, Y.Y. Chen, J. Collolid Interf. Sci. **236**, 41(2001).
[2] C. Liu, B.S. Zou, A.J. Rondinone, Z.J. Zhang, J. Am. Chem. Soc. **122** , 6263 (2000).
[3] Yen-Pei Fua, Dung-Shing Hung, Yeong-Der Yao, Ceram. Int. **35**, 2179 (2009).
[4] A. Berkovitz, W.T. Schuele, Journal of Applied Physics. **30,** 134 (1959).
[5] R.W. McCallum, K.W. Dennis, D.C. Jiles, J.E. Snyder, Y.H. Chen, Low Temperature Physics **27**, 266 (2001).
[6] Y. Chen, J.E. Snyder, C.R. Schwichtenberg, K.W. Dennis, R.W. McCallum, D.C. Jiles, IEEE Transactions on Magnetics **35**, 3654 (1999).
[7] T.J. Shinde, A.B. Gadkari, P.N. Vasambekar , Journal of Magnetism and Magnetic Materials **322**, 2777 (2010).
[8] M.A. Khan, M.U. Islam, M. Ishaque, I.Z. Rahman , Ceramics International **37**(7)**,** 2519 (2011).
[9] E. Rezlescu, N. Rezlescu, P.D. Popa, L. Rezlescu, C. Pasnicu, Physica Status Solidi A **162**(2), 673 (1997).
[10] M.A. Ahmed, N. Okasha, M.M. El-Sayed, Ceramics International **33 (1),** 49 (2007).
[11] K.K. Patankar, S.S.Joshi, B.K. Chougule, Physics Letters A **346**, 337 (2005).
[12] S.L. Kadam, K.K. Patankar, C.M. Kanamadi, B.K. Chougule, Materials Research Bulletin **39**, 2265(2004).
[13] F. Cheng, C. Liao,J. Kuang, Z. Xu, C. Yan, L. Chen, H. Zhao, Z. Liu , Journal of Applied Physics **85,** 2782(1999).
[14] N. Rezlescu, E. Rezlescu, C. Pasnicu, M.L. Craus, Journal of Physic Condensed Matter **6,** 5707(1994).
[15] N. Rezlescu, E. Rezlescu, Solid State Communications **88**, 139 (1993).
[16] S. Dwevedi, K.K. Bharathi, G. Markandeyulu, IEEE Transactions on Magnetics

45, 4253 (2009).
[17] A.B. Gadkari, T.J. Shinde, P.N. Vasambekar , Mater. Chem. Phys. **114**, 505 (2009).
[18] M.A.L. Haj, Turk.J. Phys. **28**, 391 (2004).
[19] N. Rezlescu, E. Rezlescu, C.L. Sava, F. Tudorache, P.D. Popa, Phys. Stat. Sol. (a). **201 (1)**, 17 (2004).
[20] O.M. Hameda, M.Z. Said, M.M. Barakat, J. Magn. Magn. Mater. **224,** 132 (2001).
[21] K.H. Wu, T.H. Ting, M.C. Li, W.D. Ho, J. Magn. Magn. Mater. **298**, 25 (2006).
[22] C.W. Kim, J.G. Koh , J. Magn. Magn. Mater. **257**, 355 (2003).
[23] M.S. Hegde, D. Larcher, L. Dupont , Solid State Ion **93**, 33 (1997) .
[24]Ge-Liang Sun, Jian-Bao Li, Jing-Jing Sun and Xiao-Zhan Yang , JMMM. **281**, 173 (2004).
[25] Gul, I.H. and A. Maqsood, Journal of Alloys and Compounds **465**, 227 (2008).
[26] A.A. Kadam, S.S.Shinde, S.P.Yadav, P.S.Patil and K.Y.Rajpure, Journal of Magnetism and Magnetic Materials **329**, 59 (2013).
[27] Ishtiaq Ahmad and Muhammad Tahir Farid, World Applied Sciences Journal **19**(4), 464 (2012).
[28] Lanje, N.Y. and D.K. Kulkarni, JMMM. **234**, 114(2001).
[29] Manisha, V. Rane, D. Bahadur, A.K Nigam and C.M. Srivastava, JMMM. **192**, 288(1999).
[30] D.S. Birajdar, D.R. Mane, S.S. More, V.B. Kawade, K.M.Jadhav, J. Mater. Lett. **59**, 2981(2005).
[31] L. Nalbandian, A. Delimitis, V.T. Zaspalis, E.A. Deliyanni, D.N. Bakoyannakis, E.N. Peleka, J. Micropor. Mesopor. Mater. **114**, 465 (2008).
[32] M.K. Shobanaa, S. Sankara, V. Rajendranb, Mater. Chem. Phys. **113**, 10 (2009).
[33] Tatina N. brusentosva, Viatcheslva D. kuznetsov, J. Magn. Magn. Mater. **31**, 22 (2007).
[34] T.M. Meaza, S.M. Attiab, A.M. Abo El Ataa, J. Magn. Magn. Mater. **257**, 296 (2003).
[35] M. Asif Iqbal, M.U. Islam, Irshad Ali, Muhammad Azhar khan, Imran Sadiq and Ihsan Ali, Journal of Alloys and Compounds **586**, 404 (2014) .
[36] Chandra Babu.B,Naresh. V, Jayaprakash. B, S. Buddhudu , Ferro Electrics letter **38**, 124 (2011).
[37] N. Rezlescu, E. Rezlescu, Physics Status Solidi A. **23**, 575 (1974).
[38] I.H. Gul, A. Maqsood, M. Naeem, M. Naeem Ashiq, Journal of alloys and compounds **507**, 201 (2010).
[39] K.W. Wagner, American Physics **40**, 317 (1973).
[40] Muhammad Tahir Farid, Ishtiaq Ahmad And Salma Aman, J. Chem. Soc. Pak. **35**, 793 (2013).
[41] B. Baruwati, K.M. Reddy, V. Sunkara, R.K. Manorama, O. Singh, J. Prakash , Applied Physics Letters **14**, 85 (2004).
[42] Devan RS, Chougule BK, Journal of Applied Physics **101**, 014109 (2007).